REGULAR ARTICLE

Fabrication of Glass/Jute Hybrid Composite over Wrapped Aluminum Cylinders: An Advanced Material for Automotive Applications

Marwa A. Abd El-baky[1] · Mahmoud M. Awd Allah[1] · Madeha Kamel[2] · Walaa Abdel-Aziem[1]

Abstract

As a class of promising cost-effective lightweight structures, metal-composite hybrids have rapidly emerged in automotive industry largely attributable to their outstanding multifunctional and crashworthy characteristics. The aim of this study is to investigate the potentiality of metal-composite cylinders for crash energy absorption applications. In this context, the crashworthiness performance, and the deformation history of jute (J)/glass (G) reinforced epoxy hybrid composite over wrapped aluminum (Al) cylinders were experimentally studied under quasi-static axial loading. Crashworthiness characteristics of the proposed cylinders were evaluated by measuring the average and peak crushing loads (F_{avg}, F_{ip}), specific energy absorption (SEA), total absorbed energy (U), and crush force efficiency (CFE). The influence of the number of J-layers on the deformation profiles has also been defined. Result revealed that the highest (F_{ip}), (F_{avg}), and (SEA) noted for Al-3G-2 J-3G with values of 85.45 kN, 53.14 kN, and 39.99 J/g, respectively. The maximum (U) was documented for Al-8G with a value of 3535.89 J. The highest (CFE) was recorded for Al-2G-4 J-2G followed by Al-3G-2 J-3G with a value of 0.65 and 0.62, respectively. Al-3G-2 J-3G cylinders exhibit excellent energy-absorbing capacity and could be applied as energy-absorbing crashworthiness structures in automotive applications.

Keywords Crashworthiness · Jute/glass hybrid composite · Aluminum (Al) cylinders · Quasi-static axial loading

1 Introduction

Crashworthiness refers to the ability of a vehicle to withstand collisions with minimal injury or damage to human bodies or cargos, which is closely associated with the structural design and material selection [1–3]. Thin-walled structures are commonly used as crashworthy components because of their benefits, including high energy-absorbing capacity (EAC), high stiffness, high strength, high corrosion resistance, low weight, low cost, and simplicity of manufacture [4–6]. For energy absorption purposes, a variety of materials can be employed. Because of their extraordinary lightweight and good specific mechanical characteristics, fiber reinforced polymer composites (FRPCs) have been attracted a lot of interest as energy-absorbing structures.

EAC of thin-walled composite structures are deemed superior to those of traditional metals, such as aluminum (Al) and mild steel, in terms of crashworthiness, giving an effective solution to fulfill the ever-increasing safety and environmental criteria [7–9].

Despite their remarkable load-bearing and lightweight properties, FRPCs have several flaws that limit their application as energy-absorbing components in vehicle industry. The limitations of FRPCs include the high cost, brittleness, and unstable failure mechanisms. As a consequence, it is more typically employed in hybrid forms, in which metal-composite hybrid constructions combine the stability, ductility, and plasticity of metals with high strength/stiffness to weight ratio of composites for crashworthy vehicle structures [10]. Several researchers have examined the crashworthiness of metals [11–14] and FRPCs [15, 16].

Several investigators studied the collapse performance of composite over metal hybrid cylinders. Babbage and Mallick [17] experimentally studied the static axial crushing response of filament-wound E-glass/epoxy over wrapped Al pipes. Fiber angle was ± 45° or ± 75° relative to the axis of the pipe. Round and square cross sections were used. Some

✉ Marwa A. Abd El-baky
dr.marwa2013@yahoo.com

1 Mechanical Design and Production Engineering Department, Zagazig University, Zagazig 44519, Egypt

2 Mechanical Engineering Department, Suez Canal University (SCU), Ismailia, Egypt

cylinders were filled with epoxy foam. Results indicated that as the number of E-glass layers increase the crashworthiness parameters values increase. Crashing parameters of round cylinders are better than those of square ones. $\pm 45°$ orientation angle gives better crashing parameters than those of $\pm 75°$. Kalhor and Case [18] observed that wrapping of S2 glass/epoxy over 304 stainless steel square cylinders can alter its failure mode from splitting with low absorbed energy (U) to symmetric or mixed mode with higher U and more stability. The number of the composite layers have a considerable influence on U.

Liu et al. [19, 20] found that peak crushing load (F_{ip}) and U of the filled carbon reinforced plastic (CFRP)/Al honeycomb structures increase by 10% compared with CFRP hollow structures. With decreasing Al honeycomb unit length, U increases while specific energy absorption (SEA) decreases. Zhu et al. [21] studied the crushing performance and collapse modes of three configurations of Al/CFRP hybrids under quasi-static axial loads. For comparison purpose, empty Al and CFRP cylinders were tested. Results indicated that H-I (Al cylinder internally filled with CFRP cylinder) offers the best crashworthiness characteristics.

Sun et al. [22] noticed that the winding angle and wall thickness in Al/CFRP have a considerable effect on collapse modes and crushing indicators of CFRP and hybrid cylinders. With constant laminate thickness, increasing the winding angle decreases SEA, U and F_{ip} of CFRP and hybrid cylinders. With constant winding angle of CFRP, increasing the thickness of CFRP cylinder increases SEA, U and F_{ip} of CFRP and hybrid cylinders. SEA of CFRP cylinder with nine-ply and 25° winding angle and CFRP/Al hybrid cylinder with nine-ply and 25° winding angle are the highest with values of 48.74 and 79.05 J/g, respectively.

A perfectly designed hybrid metal-composite cylindrical structures with suitable reinforcement have been proved to be lighter and safer than traditional metallic or composite cylinders. This supports hybrid metal-composite cylindrical structures to be adapted as a superior option in crashworthiness applications, Mahdi and El Kadi [23]. Researchers tried to mitigate the utilization of expensive synthetic fibers by employing low density natural cellulosic fibers to reduce the overall weight, Supian et al. [24]. Cellulosic fibers such as kenaf, ramie, flax, and jute have been adapted in structural applications due to their biodegradability, low cost, high specific strength, and eco friendliness, and readily availability [25–27]. Various researchers have studied the crashworthiness and collapse performance of natural fiber reinforced composites [28–31].

It is worth noting that in exhaustive investigations have been carried out on synthetic/natural hybrid composite over wrapped metallic cylinders. So, the main objective of the present study is to experimentally investigate the influence of hybridization process and the number of J-layers on the crashworthiness and collapse performance of jute (J)/glass (G) hybrid composites over wrapped Al cylinders fabricated using wet warping by hand lay-up technique and tested under quasi-static axial loading. The potentiality of using jute, glass fibers with Al cylinders for crash energy absorption applications was investigated.

2 Methodology

The influence of hybridization on the crashworthiness performance of Al-Jute (J)-Glass (G) reinforced epoxy circular hybrid composite cylinders was investigated using uniaxial quasi-static crushing tests.

2.1 Materials

Plain weave E-glass and jute fabrics with GSM of 200 g/m^2 were chosen as reinforcements. E-glass and jute fabrics were supplied by Hebei Yuniu Fiber Glass Manufacturing Co. Ltd., China Mainland. and Hangzhou Zhong Xing Cotton and Jute Co. Ltd. (Zhejiang, China, Mainland), respectively. Al alloy used in this work is Al6063 in the form of cylinders with 50 mm outer diameter and 2 mm thickness, provided by Military Production Co. Ltd. (Egypt). The cause for using Al6063 tubes is its obtainability, low weight, low cost, high inherent extrudability, high strength and ductility. This alloy has several advantages, especially when weight reduction in transport systems is essential. An important characteristic of this alloy is its extremely high strength to weight ratio directly associated with fuel consumption and reduction of CO_2 emissions [32, 33]. Recently, many researchers adapted Al6063 in their studies and recommended it in crashworthiness applications, [34, 35]. Kemapoxy 150RGL supplied by Chemicals for Modern Buildings Co. Ltd., Egypt was selected as a matrix material. Table 1 demonstrates the mechanical properties of E-glass, jute, Al6063, and Kemapoxy 150 RGL. The chemical composition of Al6063 (wt. %) is declared in Table 2.

Table 1 The properties of reinforcements and matrix given by the supplier

Property	E-glass	jute	Al6063	Kema-poxy 150 RGL
Density, g/cm^3	2.5	1.35	2.7	1.1
Young's modulus, GPa	76	17	68.9	1.2
Elongation, %	1.8–3.2	1.5–1.8	18–33	2.2–2.9
Tensile strength, MPa	3400	470	186	55–58

Table 2 Al 6063 chemical composition (weight percentage)	Si	Fe	Cu	Mn	Mg	Zn	Ti	Al
	0.44	0.18	0.01	0.04	0.48	0.01	0.01	Bal

2.2 Surface Treatment of Al Cylinders

Mechanical and chemical treatments were accomplished on Al-alloy cylinders to guarantee the appropriate bond between Al cylinders, jute, and E-glass fabrics. Mechanical treatment was performed by rinsing Al cylinders with acetone and roughening them smoothly with # 400 grit sandpaper, then washing the cylinders with distilled water and finally drying the cylinders in an oven. Chemical treatment was performed on the mechanically treated cylinders by acid washing using HCl having 11% volumetric concentration to increase Al cylinder surface roughness. Acid etching was achieved at an ambient temperature for 30 min. Al cylinders were rinsed with distilled water and dried out. Al cylinders were immersed in a 5 wt. % NaOH solvent for 5 min at 70 °C. The oxidized Al cylinders were dried in an oven to stabilize the oxide layer and washed with tap water to remove the oxide residue [36].
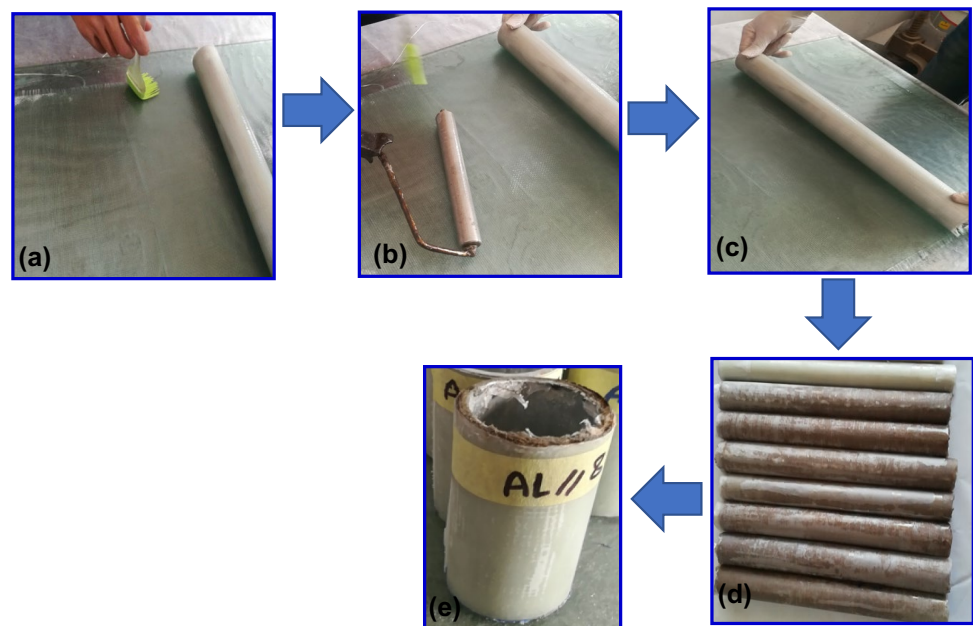
2.3 Fabrication of Hybrid Composite Specimens

Test specimens were prepared via wet wrapping by hand lay-up method. Because of its ease and low arrangement necessities, this method was selected. Each metal-composite cylinder was made up of eight plies wound around an Al cylinder. Many researchers summarized the steps of the fabrication process [2, 8, 37, 38]. Figure 1 shows the steps of the fabrication method, which can be described as follows:

- According to the supplier's guidelines and technical data sheets, epoxy and its hardener were mixed in 2:1 weight ratio. The mixture was then stirred for about 5 min before being used. The mixture was evenly applied to the fabric with a manual brush, as shown in Fig. 1(a). The fabric was impregnated with matrix using a roller. Figure 1(b).
- The saturated fabric was then wrapped around a 50 mm outer diameter circular Al cylinder, as shown in Fig. 1(c). After that, the primarily formed cylinder was covered with caulk paper.
- The initial curing period of the primarily fabricated cylinders was 24 h at 25 °C. It took 7 days for the cylinders to extent their full hardness and shrinking potential.
- The produced cylinders were examined after curing for any geometrical irregularities or material faults. The finished product is shown in Fig. 1(d).
- Cylinders with 100 ± 4 mm lengths were cut, Fig. 1(e). Table 3 summarizes the test specimen codes, and other information for test specimens.
- The main point of comparison between the composite/Al specimens is the constant number of composite plies. Each metal-composite cylinder was made up of eight plies wound around an Al cylinder. Geometrical descrip-

Fig. 1 Fabrication steps of Al/GFRP composite tubes

Table 3 Geometrical descriptions of the fabricated metal-composite hybrid cylinders

Specimen code	Average specimen thickness (t), mm	Average specimen length (L), mm	Average specimen mass (M), g
Net Al	2.00	97.40	96.20
Al-8 J	8.60	99.35	161.08
Al-1G-6 J-1G	7.68	98.12	150.19
Al-2G-4 J-2G	6.54	102.34	138.76
Al-3G-2 J-3G	4.91	99.66	132.43
Al-8G	4.06	96.59	125.50

The letters "Al", "J" and "G" in the specimen code represent aluminum tube, jute fiber plies and, glass fiber plies, respectively. For example, "Al-1G-6 J-1G" mean that "1" glass fiber ply, "6" jute fiber plies, and "1" glass fiber ply over wrapped aluminum cylinder

tions of the fabricated metal-composite hybrid cylinders are summarized in Table 3.

It is clear from Table 3 that the weight of jute/epoxy/Al composites is higher than the weight of glass/epoxy/Al. This is because jute fiber absorbs more amount of epoxy than glass fiber, which leads to increasing the weight of jute/epoxy/Al composite.

2.4 Testing

A universal testing machine with a capacity of 100 kN (Type: Jinan WDW, China (Mainland)) was used to perform a quasi-static axial compression test on Al-J-G reinforced epoxy circular hybrid composite cylinders with a crosshead speed of 10 mm/min. Prior to the start of the test, test specimens were placed between two flat steel plates that were parallel to each other. An automatic data gathering system was directly built to capture load–displacement data. Test specimen deformation histories were also tracked and reported. For each case, three specimens were tested, and the average was provided. The load–displacement curves produced can be used to quantify the performance of crashworthy metal-composite specimens. The following are the crushing critical parameters: initial peak crash load (total absorbed energy (U), specific absorbed energy (SEA), mean crash force (F_{avg}) and crashing force efficiency (CFE).

- Initial peak force (F_{ip}) can be directly recorded from the crushing load–displacement curve. It is advised that it be small enough to prevent the energy absorber from transferring the crashing force to the main vehicle body.
- Total absorbed energy (U) indicates the amount of energy lost during the crushing process. It is numerically defined as:

$$U = \int_0^{\delta_{max}} F(\delta)d\delta \tag{1}$$

where, $F(\delta)$ and δ_{max} are the instantaneous crushing force and total crush displacement, respectively.

- Average crash force (F_{avg}) can be attained by the total energy absorption divided by total crush displacement.

$$F_{avg} = \frac{\int_0^{\delta_{max}} F(\delta)d\delta}{\delta_{max}} \tag{2}$$

- Crashing force efficiency (CFE) is the ratio of average crash force to first peak crash force in percent. When the crashing force efficiency percentage is high, the structure's effective EAC is also high.

$$CFE = \frac{F_{avg}}{F_{ip}} \times 100 \tag{3}$$

- Specific absorbed energy (SEA) is the energy absorbed (U) divided by the mass of the energy absorber (m_c):

$$SEA = \frac{U}{m_c} \tag{4}$$

$$m_c = \left(\frac{M}{L}\right)\delta_{max} \tag{5}$$

where, M/L is the pretest energy absorber structure per unit length.

3 Results and Discussions

3.1 Load–Displacement Curves and Crushing History

Load–displacement and energy absorption curves for glass/jute hybrid composite over wrapped Al configurations are shown and explained in detail in the following sections. Each load–displacement curve is correlated with the representative specimen deformation histories for convenience in viewing the failure progress. Generally, it was noted from Figs. 2–7 that the behaviors of all fabricated cylinders are nearly linear till they come up to the first peak load then a load drop can be recorded. The magnitudes of the first peak load and load drop are controlled by the number of jute and glass layers incorporated in the cylinder. A load fluctuation around the average crushing load in the post crushing stage was observed for all tested cylinders. Then an increase in the load was noticed by way of the compaction zone was

Fig. 2 Load–displacement and crushing history for net Al test specimen

(a)

(b)

| 0 mm | 3.97 mm | 20.28 mm | 42.05 mm | 60.53 mm | 79.41 mm |
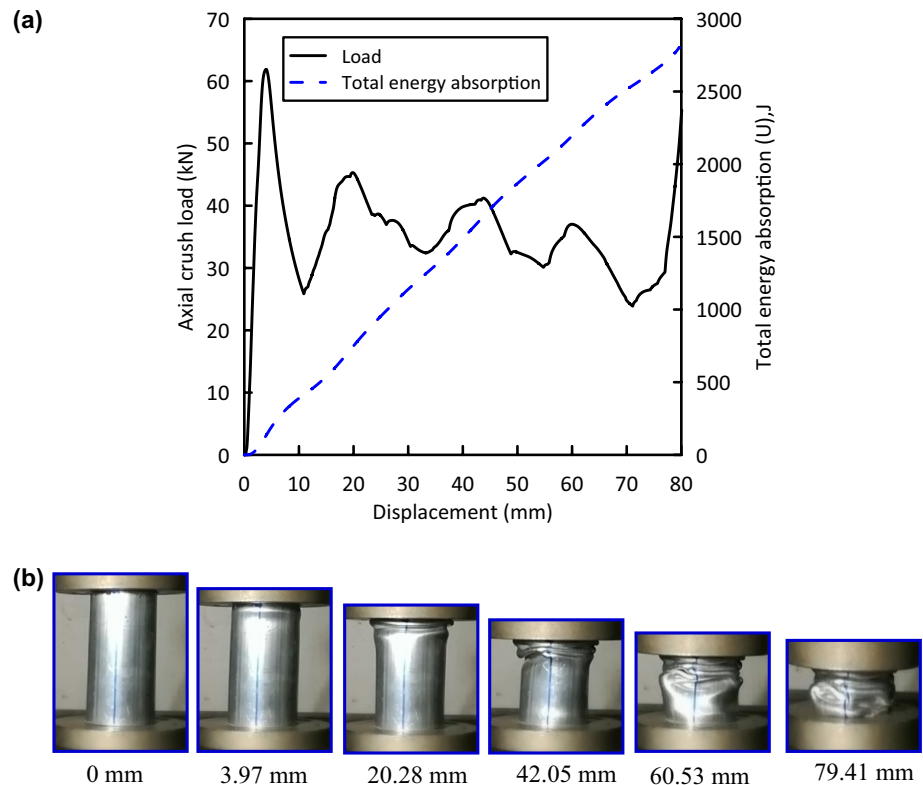
reached as the table of the machine holds the specimen and withstands the force which quickly rises. This result agrees with that attained by Abdewi et al. [39] and Alshahrani et al. [35, 40].

3.1.1 Pure Al Specimen

Figure 2 shows load–displacement curve, energy absorption-displacement curves and crushing history for the most representative Al cylinder sample. It is clear from Fig. 2(a) that pure Al-specimen behaves linear till it approaches the first peak value of 61.87 kN at 3.97 mm followed by a sharp load drop to about 25.23 kN at 10.32 mm. With increasing the crushing displacement, pure Al-specimen gradually deforms plastically and yields load–displacement profile with high oscillations' amplitude in post crashing zone till it reaches the beginning of the compaction zone at about 79.41 mm. It is clear from Fig. 2(a) that the energy absorption increases linearly with the displacement. Figure 2(b) shows the crushing history for pure Al test specimen. Wrinkling and global buckling of the cylinder walls can be noted.

3.1.2 Al-8 J Specimen

Figure 3 shows load–displacement curve, energy absorption-displacement curves and crushing history for the most representative Al-8 J cylinder sample. It is clear from Fig. 3(a)

that Al-8 J specimen behaves linear till it approaches the first peak value of 80.88 kN at 8.06 mm, followed by a load drop to about 49.65 kN at 18.56 mm. The load drop is accompanied with matrix fretting and interlaminar cracks starting to occur at the top the cylinder due to the local stress concentration. After load drop, the load–displacement curve slightly oscillated in the post crushing zone till it reaches the beginning of the compaction zone at 64.65 mm. At the beginning of the compaction zone, the axial load increases rapidly. Figure 3(a) shows that the energy absorption increases nonlinearly with the displacement. Bending, wrinkling, and global buckling of the cylinder walls can be noted due to the buckling of the fiber, Fig. 3(b).
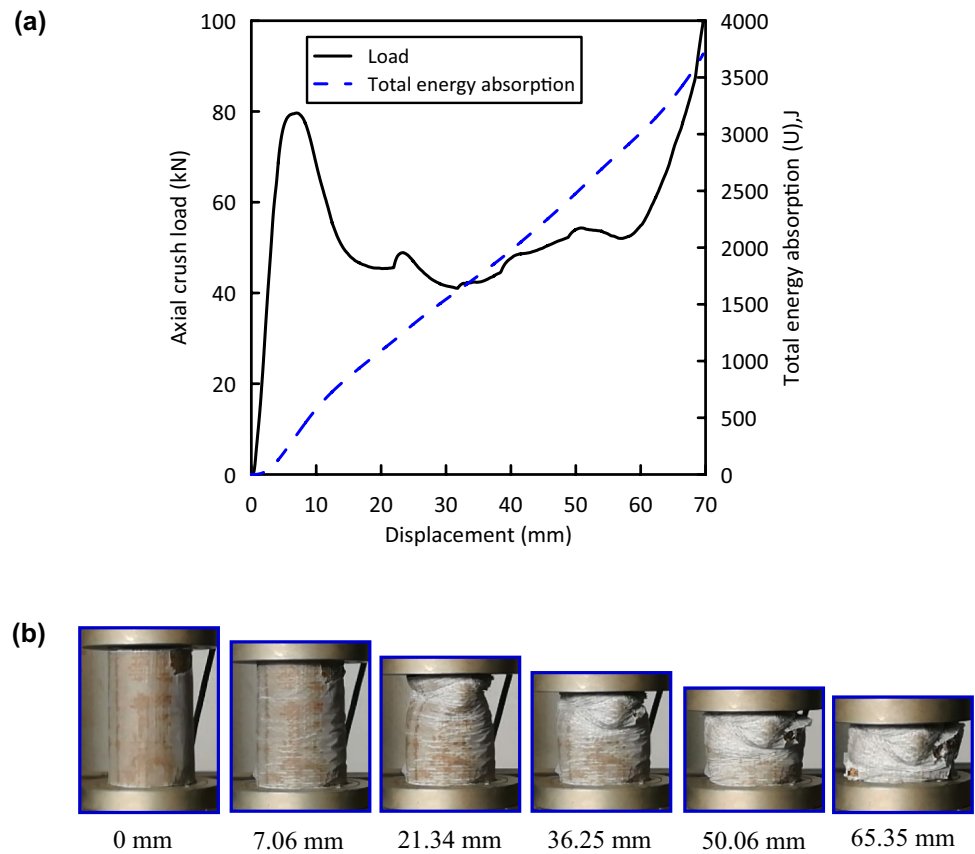
3.1.3 Al-1G-6 J-1G Specimen

Figure 4 displays the load–displacement response and crushing history for the most representative Al-1G-6 J-1G specimen tested under quasi-static loading. It is clear from Fig. 4 that the cylinder behaves linearly till it approaches the first peak load of 79.66 kN at 7.06 mm, followed by a sharp load drop to about 47.45 kN at 14.25 mm. After that, low fluctuation in the post crushing zone can be observed till the beginning of the compaction zone at 65.35 mm. It is obvious from Fig. 4(a) that the energy absorption increases in a nonlinear manner with the displacement. Wrinkling, wall bending, and

Fig. 3 Load–displacement and crushing history for Al-8 J test specimen

(a)

(b)

0 mm　　8.06 mm　　22.47 mm　　39.36 mm　　52.66 mm　　64.65 mm
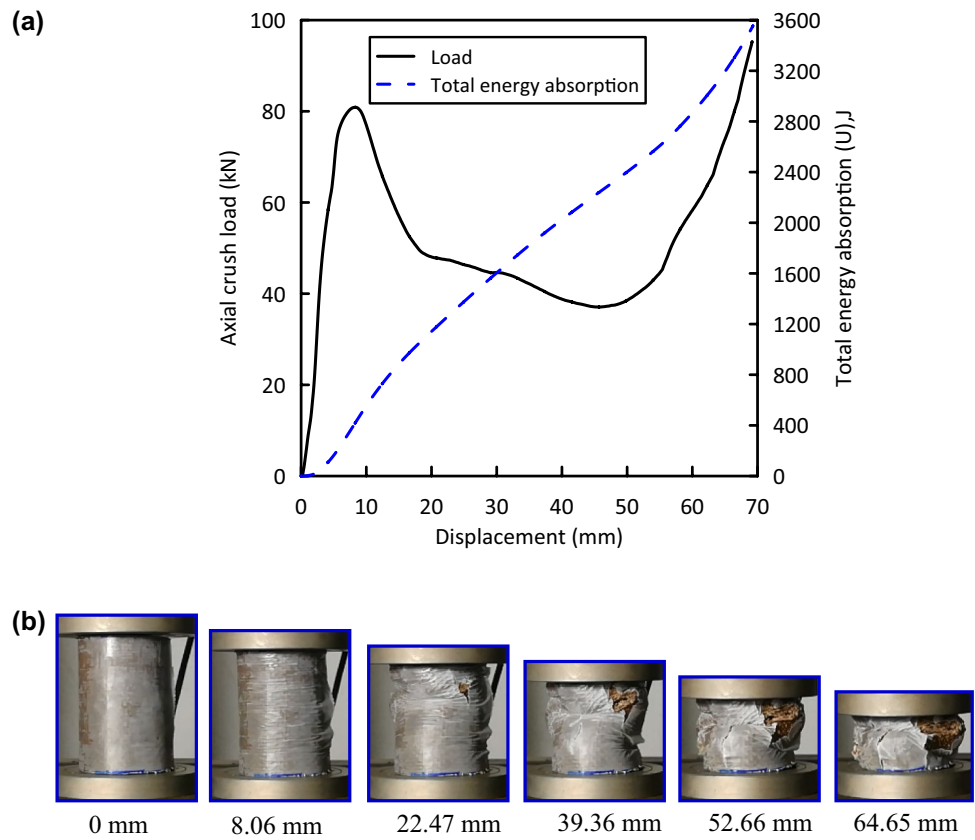
Fig. 4 Load–displacement and crushing history for Al-1G-6 J-1G test specimen

(a)

(b)

0 mm　　7.06 mm　　21.34 mm　　36.25 mm　　50.06 mm　　65.35 mm

global buckling accompanied with cracking at the top and bottom of the cylinder can be noticed.

3.1.4 Al-2G-4 J-2G Specimen

Figure 5 shows the load–displacement response and crushing history for the most representative Al-2G-4 J-2G specimen obtained from the quasi-static axial compression test. The cylinder behaves linearly till it approaches the first peak load of 81.29 kN at 8.59 mm, followed by a sharp load drop at about 20.89 kN. After load drop, the load–displacement curve oscillated in the post crushing zone till it reaches the beginning of the compaction zone at 70.29 mm, Fig. 5(a). Nonlinear trend was noticed for energy-displacement curve. Matrix cracking at the bottom of the cylinder can be noticed as shown in Fig. 5(b).
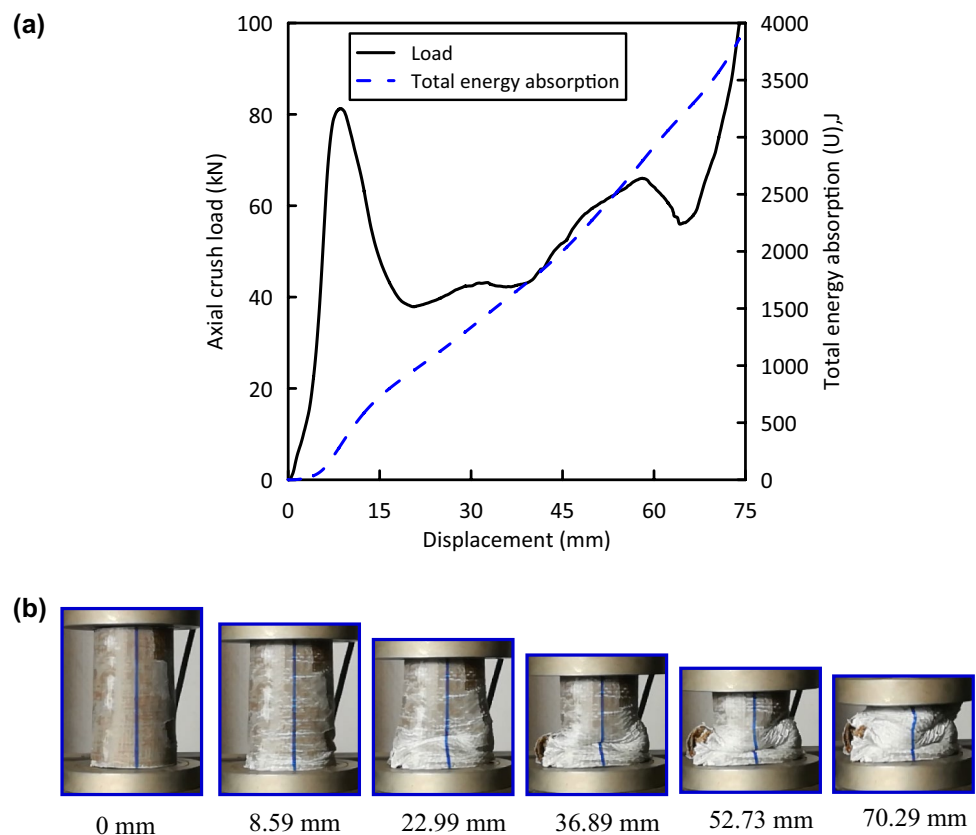
3.1.5 Al-3G-2 J-3G Specimen

Load–displacement response and crushing history obtained from the quasi-static axial compression test for the most representative Al-3G-2 J-3G cylinder are shown in Fig. 6. It was noticed that the cylinder behaves linearly till it approaches the first peak load of 85.45 kN at 5.240 mm, followed by a sharp load drop to about 38.305 kN at 18.22 mm. After load drop, the load–displacement

curve oscillated in the post crushing zone till the cylinder reaches the beginning of the compaction zone at 64.92 mm, Fig. 6(a). Nonlinear trend for the energy-displacement behavior can be recorded, Fig. 6(a). Delamination in the specimen wall accompanied with longitudinal cracks can be noticed, Fig. 6(b).

3.1.6 Al-8G Specimen

Load–displacement response and crushing history obtained from the quasi-static axial compression test for the most representative Al-8G specimen are shown in Fig. 7. It was observed that the cylinder behaves linearly till it moves toward the first peak force of 77.54 kN at 4.95 mm, followed by a sharp load drop to about 32.31 kN at 18.37 mm. After load drop, the load–displacement curve oscillated in the post crushing zone till the beginning of the compaction zone at 72.00 mm. Nonlinear behavior for energy-displacement curve can be recorded, Fig. 7(a). Global buckling with fiber fracture were noticed for Al-8G specimen, Fig. 7(b). It is clear from Figs. 2–7 that the magnitudes of the first peak load and load drop are controlled by the number of jute and glass layers incorporated in the cylinder.

Fig. 5 Load–displacement and crushing history for Al-2G-4 J-2G test specimen

Fig. 6 Load–displacement and crushing history for Al-3G-2 J-3G test specimen

0 mm 5.24 mm 16.92 mm 33.43 mm 51.26 mm 64.92 mm
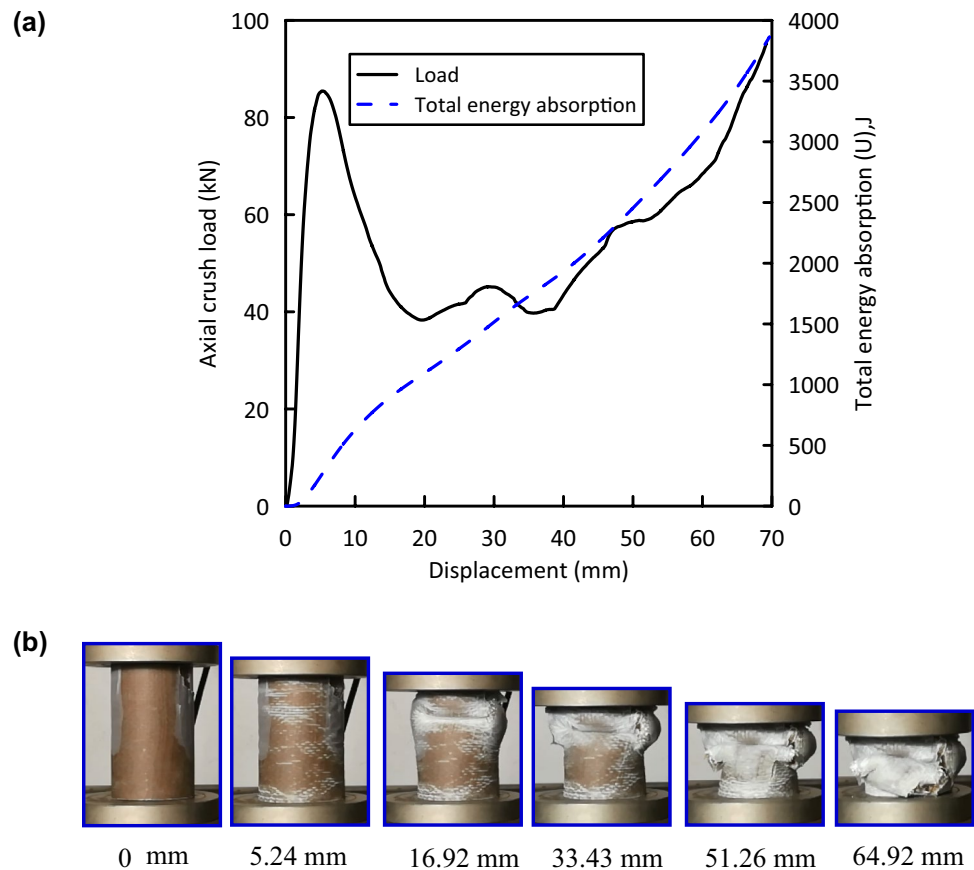
3.2 Crashworthiness Parameters

3.2.1 Initial Peak Load $\left(F_{ip}\right)$ and Average Load $\left(F_{avg}\right)$

As shown in Table 4, the lowest initial peak load (F_{ip}) was recorded for Al cylinder with a value of 61.87 kN. Hybridizing Al cylinder with eight layers of jute/epoxy, and glass/epoxy gives an enhancement of, respectively, 30.73 and 28.56% in F_{ip} of Al cylinder. F_{ip} of Al-1G-6 J-1G, Al-2G-4 J-2G, and Al-3G-2 J-3G cylinders are, respectively, about 1.29, 1.31, and 1.38 times that of Al cylinder. This is due to the increasing in the wall thickness of the tubes. This result agrees with that obtained by Mirzaei et al. [41]. This means that hybridizing Al with jute and glass has a visible positive effect on the value of F_{ip}. Hybridizing Al cylinder with eight layers of jute/epoxy, and glass/epoxy gives an enhancement of, respectively, 38.91 and 39.68% in F_{avg} of Al cylinder. F_{ip} of Al-1G-6 J-1G, Al-2G-4 J-2G, and Al-3G-2 J-3G cylinders are, respectively, about 1.42, 1.50, and 1.51 times that of Al cylinder. This means that hybridizing Al with jute and glass has a visible positive effect on the value of F_{avg}.
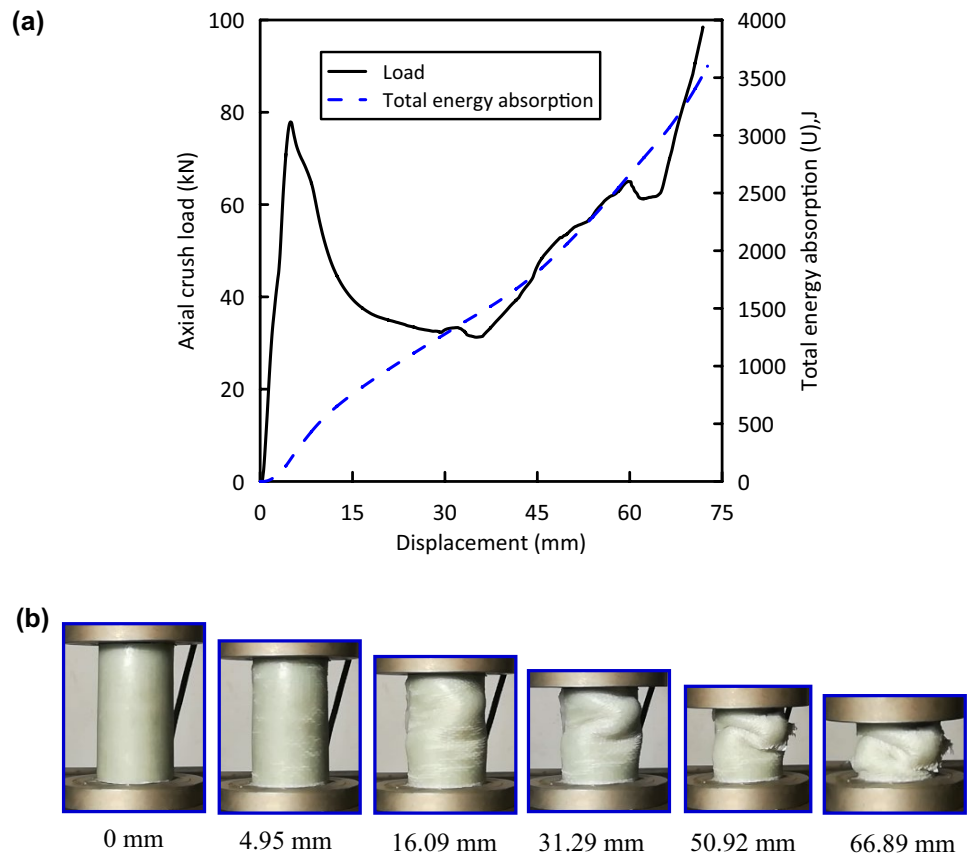
3.2.2 Crush Force Efficiency (CFE)

As represented in Table 4. The highest CFE value was recorded for Al-2G-4 J-2G cylinder with a value of about 0.65, whereas the lowest CFE was detected for Al cylinder with a value of about 0.57. Hybridizing Al cylinder with eight layers of jute/epoxy, and glass/epoxy gives an enhancement of, respectively, 5.26 and 8.77% in CFE of Al cylinder. CFE of Al-1G-6 J-1G, Al-2G-4 J-2G, and Al-3G-2 J-3G cylinders are, respectively, about 1.09, 1.14, and 1.09 times that of Al cylinder. This means that hybridizing Al with jute and glass has a visible positive effect on the value of CFE.

3.2.3 Total Absorbed Energy (U)

As represented in Table 4, the highest energy absorption (U) was recorded for Al-8G cylinder with a value of about 3535.89 kJ, whereas the lowest (U)was observed for Al cylinder with a value of about 2791.84 kJ. This means that wrapping glass/epoxy layers over pure Al cylinder has an enhancement of 23.56% in (U) compared with pure Al

Fig. 7 Load–displacement and crushing history of the Al-8G test specimen

(a)

(b)

| 0 mm | 4.95 mm | 16.09 mm | 31.29 mm | 50.92 mm | 66.89 mm |

Table 4 Crashworthiness parameters of metal-composite hybrid cylinders

Specimen code	Initial peak crash force F_{ip}, kN	Total energy absorption U, J	Mean crash force F_{avg}, kN	Crashing force efficiency CFE	Specific energy absorption SEA, J/g
Net Al	61.87	2791.84	35.16	0.57	35.60
Al-8 J	80.88	3157.77	48.84	0.60	30.13
Al-1G-6 J-1G	79.66	3252.50	49.77	0.62	32.52
Al-2G-4 J-2G	**81.29**	3391.88	**52.84**	**0.65**	**38.97**
Al-3G-2 J-3G	**85.45**	3449.69	**53.14**	**0.62**	**39.99**
Al-8G	79.54	**3535.89**	49.11	0.62	37.80

cylinder. This result is consistent with results obtained by Kalhor and Case [18] for 304 stainless steel square cylinders over wrapped by of S2 glass/epoxy. Also, (U) value of Al-8 J cylinder is shown in Table 4 with value of about 3157.77 kJ which presents 1.13 times that of Al cylinder. (U) of Al-1G-6 J-1G, Al-2G-4 J-2G, and Al-3G-2 J-3G cylinders are, respectively, about 1.17, 1.21, and 1.24 times that of Al cylinder. This means that hybridizing Al with jute and glass has a visible positive effect on the value of (U). Increasing the number of glass layers with respect to jute layers improves (U).

3.2.4 Specific Absorbed Energy (SEA)

As demonstrated in Table 4, the highest specific energy absorption (SEA) value was recorded for Al-3G-2 J-3G cylinder with a value of about 39.99 kJ/g, whereas the lowest (SEA) was observed for Al-8 J cylinder with a value of about 30.13 kJ/g. Wrapping eight layers of glass/epoxy over Al cylinder improves (SEA) by 6.18%. (SEA) of Al-1G-6 J-1G, Al-2G-4 J-2G, Al-3G-2 J-3G, and Al-8G cylinders are, respectively, about 1.08, 1.29, 1.33, and 1.25 times that of Al-8 J cylinder. It is clear from Table 4 that wrapping hybrid

jute/glass reinforced epoxy layers over Al cylinder improves SEA of Al cylinders. This result is consistent with that obtained by Alshahrani et al. [35]. Sun et al. [22] proved that increasing the wall thickness of Al/CFRP cylinder, which consequently increases the rigidity of the cylinder, increases SEA, U and F_{ip} of hybrid cylinders.

3.3 Failure Mechanisms

Energy absorbers are generally designed to absorb maximum crush energy. Failure mechanism is a significant parameter to investigate energy absorbing capacity of

metal-composite hybrid cylinders [42]. Photos of top views for the crushed specimen are shown in Fig. 8. Two failure modes were observed. They can be classified as follows:

Mode I: Axisymmetric or ring mode was recorded for the net Al-specimen.

Mode II: Hybrid cylinders were initially buckled and matrix macro-cracks' formation was noticed. Then, the cracks propagate in the cylinder peripheral direction. Further propagation of the cracks causes lamina bending, formation of internal and external folds. Also, delamination, fiber breakage and fiber pull-out can be noticed. This phenomenon was recorded by Attia et al. [37] for hybrid tubes.

Fig. 8 Top views for the crushed specimens

Net Al **Al-1G-6J-1G** **Al-2G-4J-2G**

Al-3G-2J-3G **Al-8J** **Al-8G**
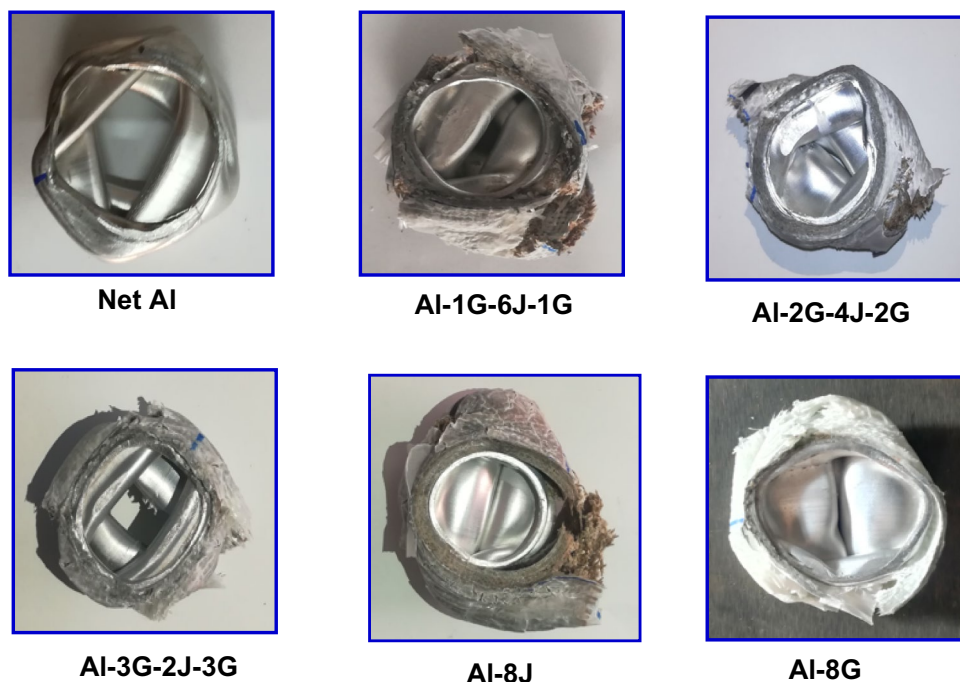
Table 5 SEA for some metallic and fiber reinforcement composite tubes (labeled in the literature)

Material of the energy absorber tube	SEA (J/g)	References
Aluminum (Al) cylinder	32.41	Zhu et al. [43]
Carbon/epoxy (CFRP)	37.82	Zhu et al. [44]
Al /CFRP hybrid tube	22.81	Zhu et al. [44]
Al cylinder internally filled with CFRP cylinder	24.57	Zheng et al. [45]
CFRP cylinder internally filled with Al cylinder	23.80	Zheng et al. [45]
Kenaf/Glass/epoxy	5.64–14.39	Supian et al. [46]
Jute/Kevlar/epoxy	15.36–26.51	Albahash and Ansari [47]
Flax/epoxy	9.68–37.16	Yan and Chouw [48]
wood	18–31.6	Guélou et al. [49]
Woven jute/epoxy	33.20	Sivagurunathan et al. [50]
Ramie/bio-epoxy	15.80	Ghoushji et al. [51]
Kenaf/epoxy	38.90	Alkateb et al. [52]
Basalt/epoxy	30.68	Roslan et al. [53]
Silk/epoxy	12.00	Oshkovr et al. [54]

3.4 Applications

Table 5 lists some previously published data in the literature for the specific energy absorption of natural/synthetic fiber reinforced epoxy and metallic energy absorbers for the purpose of evaluating the crashworthiness performance of the current innovative hybrid composite energy absorbers. It is clear from Table 5 that combining wrapping hybrid natural/synthetic fibers over Al cylinders can improves the crashworthiness performance of Al energy absorbers. In addition, as compared with traditional metals, fiber reinforced composites, and hybrid cylinders, the proposed cylinders demonstrated improved crashworthiness performance, and as a result, the innovative energy absorber can be employed as energy-absorbing components in the front of train or automobile structures i.e., anti-impact rods or a crash box and can also be adapted in aircraft fuselage. Hybrid composites into energy-absorbing devices or crash box can be designed for a particular type of load into various major structures for high-performance applications and safety equipment in major transportation industries such as aerospace, automotive and marine industry, Fig. 9.

3.5 Future Directions

The current innovative hybrid metal-composite cylinders demonstrated improved crashworthiness performance under quasi-static axial compression loading, so the next step is to investigate its behavior under other quasi-static loading (lateral and oblique) as well as dynamic loads. Investigating the effect of the induced holes on it, for facility of joining and engineering requirements are of importance.

4 Conclusions

The current study investigates the effect of hybridization on the crashworthiness behaviors and failure mechanism of metal/composite hybrid cylinders. Circular cylinders were fabricated using wet wrapping by hand lay-up process and tested under quasi-static axial compression loading. The following observations have been documented:

- Hybridization process has a significant effect on the crashworthiness performance and failure mechanisms. Hybridization of Al cylinders with jute and glass reinforced epoxy layers leads to an increase in initial peak crash force (F_{ip}), average crash force (F_{avg}), total energy absorption (U), and crashing force efficiency (CFE).
- The highest (F_{ip}) and (F_{avg}) were recorded for Al-3G-2 J-3G with values of 85.45 and 53.14, respectively. The highest (U) was recorded for Al-8G with a value of 3535.89 J. The highest CFE was recorded for Al-2G-4 J-2G followed by Al-3G-2 J-3G with a value of 0.65 and 0.62, respectively. The highest SEA was recorded for Al-3G-2 J-3G followed by Al-2G-4 J-2G with a value of 39.99 and 38.97, respectively.
- As one of cost-effective structures, glass/jute over wrapped Al thin-walled cylinders have been recommended to be used as vehicular energy-absorbing components, such as front rails and crash boxes.
- Increasing glass to jute ratio, increasing total energy absorption (U) compared to net Al cylinders.
- Hybridizing Al cylinder with glass-jute reinforced epoxy changes the failure mechanism from axisymmetric or ring mode to buckling, matrix macro-cracks' formation, crack propagation in the cylinder's peripheral direction. Further the propagation of the cracks

Fig. 9 Safety component devices for energy absorption in automobile/train/aircraft applications
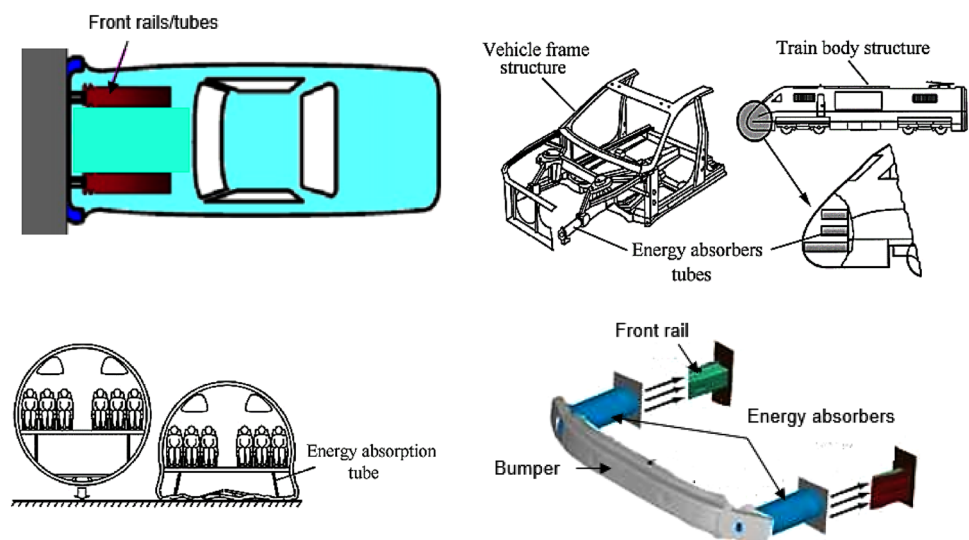
causes lamina bending and the formation of internal and external folds. Delamination, fiber breakage, and fiber pull-out can be noticed.

- Natural/synthetic fiber reinforced composites over wrapped Al cylinders are considered novel hybrid systems for energy absorption applications. This is of great significance for the application of the proposed structures in the automobile design.

Data Availability The datasets generated during and/or analyzed during the current study are available from the corresponding author on reasonable request.

Declarations

Conflict of Interest No potential conflict of interest was reported by the authors.

References

1. A. Baroutaji, M. Sajjia, A.-G. Olabi, Thin-Walled Struct. **118**, 137 (2017)
2. M.A. Abd El-baky, D.A. Hegazy, M.A. Hassan, App. Compos. Mater. **29**, 1195 (2022)
3. H. Alshahrani, T.A. Sebaey, D.A. Hegazy, M.A.A. El-baky, Poly. Advanc. Tech. **33**, 2921 (2022)
4. M.M. Awd Allah, A. Shaker, M.A. Hassan, M.A. Abd El-baky, The influence of induced holes on crashworthy ability of glass reinforced epoxy square tubes. Poly. Compos. **43**, 8322 (2022)
5. C.W. Isaac, Crashworthiness performance of green composite energy absorbing structure with embedded sensing device providing cleaner environment for sustainable maintenance. Sustain. Mater. Tech. **25**, e00196 (2022)
6. G. Zhu, G. Sun, G. Li, A. Cheng, Q. Li, Compos. Struct. **184**, 41 (2018)
7. C.W. Isaac, C. Ezekwem, Compos. Struct. **257**, 113081 (2021)
8. M.A. Abd El-baky, D.A. Hegazy, M.A. Hassan, M. Kamel, Potentiality of halloysite nanoclay on crashworthiness performance of polymer composite tubular elements. J. Compos. Mater. **56**, 1901 (2022)
9. K. Abd El-Aziz, D.A. Hegazy, M.A. Abd El-baky, Impact of montmorillonite clay on energy absorption capability of glass/

epoxy composite tubes: an experimental study. Fib. Poly. **23**, 2284 (2022)
10. G. Sun, H. Yu, Z. Wang, Z. Xiao, Q. Li, Int. J. Mech. Sci. **150**, 767 (2019)
11. D.A. Oliveira, M.J. Worswick, R. Grantab, B.W. Williams, R. Mayer, Int. J. Impact Eng. **32**, 826 (2006)
12. J.S. Qiao, J.H. Chen, H.Y. Che, Thin-Walled Struct. **44**, 692 (2006)
13. A. Eyvazian, M.K. Habibi, A.M. Hamouda, R. Hedayati, Axial crushing behavior and energy absorption efficiency of corrugated tubes. Mater. Des. (1980-2015). **54**, 1028 (2014)
14. Q. Estrada, D. Szwedowicz, J. Silva-Aceves, T. Majewski, J. Vergara-Vazquez, A. Rodriguez-Mendez, Int. J. Mech. Sci. **131–132**, 776 (2017)
15. G.C. Jacob, J.F. Fellers, S. Simunovic, J.M. Starbuck, J. Compos. Mater. **36**, 813 (2016)
16. S. Patel, V.R. Vusa, C. Guedes Soares, Crashworthiness analysis of polymer composites under axial and oblique impact loading. Int. J. Mech. Sci. **156**, 221 (2019)
17. J.M. Babbage, P.K. Mallick, Compos. Struct. **70**, 177 (2005)
18. R. Kalhor, S.W. Case, Compos. Struct. **130**, 44 (2015)
19. Q. Liu, Z. Mo, Y. Wu, J. Ma, G.C. Pong Tsui, D. Hui, Compos. Pt. B Eng. **98**, 406 (2016)
20. Q. Liu, X. Xu, J. Ma, J. Wang, Y. Shi, D. Hui, Compos. Pt. B: Eng. **118**, 104 (2017)
21. G. Zhu, G. Sun, Q. Liu, G. Li, Q. Li, Compos. Struct. **175**, 58 (2017)
22. G. Sun, S. Li, G. Li, Q. Li, Compos. Pt. B Eng. **145**, 47 (2018)
23. E.-S. Mahdi, H. El Kadi, Compos. Struct. **83**, 399 (2008)
24. A.B.M. Supian, S.M. Sapuan, M.Y.M. Zuhri, E.S. Zainudin, H.H. Ya, Def. Tech. **14**, 291 (2018)
25. M.F.M. Alkbir, S.M. Sapuan, A.A. Nuraini, M.R. Ishak, Mater. Des. **60**, 85 (2014)
26. M. Megahed, S.S. Ali-Eldin, S.M. Abd El Moezz, W.S. Abdalla, J. Compos. Mater. **54**, 3381 (2020)
27. S.S. Ali-Eldin, S.M. Abd El-Moezz, M. Megahed, W.S. Abdalla, Study of hybridization effect of new developed rice straw mat/glass fiber reinforced polyester composite. J. Natur. Fib. **18**, 1194 (2019)
28. R.A. Eshkoor, S.A. Oshkovr, A.B. Sulong, R. Zulkifli, A.K. Ariffin, C.H. Azhari, Mater. Des. **47**, 248 (2013)
29. R.A. Eshkoor, S.A. Oshkovr, A.B. Sulong, R. Zulkifli, A.K. Ariffin, C.H. Azhari, Compos. Pt. B: Eng. **55**, 5 (2013)
30. M.F.A. Alkbir, M.S.B. Salit, N.B.A. Aziz, M.R. Ishak, 2016 Lateral crushing properties of non-woven kenaf (mat)-reinforced epoxy composite hexagonal tubes. Int. J. Prec. Eng. Manufact. **17**, 965 (2016)
31. C. Lu, S. Hou, Z. Zhang, J. Chen, Q. Li, X. Han, The mystery of coconut overturns the crashworthiness design of composite materials Int. J. Mech. Sci. **168**, 105244 (2020)
32. T. Hilditch, D. Atwell, M. Easton, M. Barnett, Mater. Des. **30**, 2316 (2009)
33. Q. Estrada, D. Szwedowicz, A. Rodriguez-Mendez, M. Elías-Espinosa, J. Silva-Aceves, J. Bedolla-Hernández, O.A. Gómez-Vargas, Thin-Walled Struct. **140**, 43 (2019)
34. G. Balaji, K. Annamalai, D. Pham, An experimental and numerical scrutiny of crashworthiness variables for square column with V-notch and groove initiators under quasi-static loading. Cogent Eng. **4**, 1364118 (2017)
35. H. Alshahrani, T.A. Sebaey, M.M. Awd Allah, M.A. Abd El-baky, Quasi-static axial crushing performance of thin-walled tubes with circular hole discontinuities. Poly. Compos. **56**, 4195 (2022)
36. D. Saber, M.A. Abd El-baky, M.A. Attia, Advanced fiber metal laminates filled with silicon dioxide nanoparticles with enhanced mechanical properties. Fib. Poly. **22**, 2447 (2021)

37. M.A. Attia, M.A. Abd El-Baky, M.A. Hassan, T.A. Sebaey, E. Mahdi, Crashworthiness characteristics of carbon-jute-glass reinforced epoxy composite circular tubes. Poly. Compos. **39**, E2245 (2018)

38. M.A. Abd El-baky, D.A. Hegazy, M.A. Hassan, Novel energy absorbent composites for crashworthiness applications. J. Indust. Text. **31**, 15280837221086040 (2022)

39. E.F. Abdewi, S. Sulaiman, A.M.S. Hamouda, E. Mahdi, Thin-Walled Struct. **46**, 320 (2008)

40. H. Alshahrani, T.A. Sebaey, M.M. Awd Allah, M.A. Abd El-baky, Quasi-static axial crushing performance of thin-walled tubes with circular hole discontinuities. J. Compos Mater **56**, 4195 (2022)

41. M. Mirzaei, M. Shakeri, M. Sadighi, H. Akbarshahi, Compos. Struct. **94**, 1959 (2012)

42. A. Mamalis, D. Manolakos, G. Demosthenous, M. Ioannidis, Compos. Pt. B: Eng. **28**, 439 (1997)

43. G. Zhu, J. Liao, G. Sun, Q. Li, Int. J. Impact Eng. **141**, 103509 (2020)

44. G. Zhu, G. Sun, H. Yu, S. Li, Q. Li, Int. J. Mech. Sci. **135**, 458 (2018)

45. G. Zheng, Z. Wang, K. Song, Thin-Walled Struct. **150**, 106571 (2020)

46. A.B.M. Supian, S.M. Sapuan, M. Jawaid, M.Y.M. Zuhri, R.A. Ilyas, A. Syamsir, Fib. Poly. **23**, 222 (2021)

47. Z.F. Albahash, M.N.M. Ansari, Compos. Sci. Tech. **151**, 52 (2017)

48. L. Yan, N. Chouw, K. Jayaraman, Effect of triggering and polyurethane foam-filler on axial crushing of natural flax/epoxy composite tubes. Mater. Des. **56**, 528 (2014)

49. R. Guélou, F. Eyma, A. Cantarel, S. Rivallant, B. Castanié, Crashworthiness of poplar wood veneer tubes. Int. J. Impact. Eng. **147**, 103738 (2021)

50. R. Sivagurunathan, S. Lau Tze Way, L. Sivagurunathan, M.Y. Yaakob, The effects of triggering mechanisms on the energy absorption capability of circular jute/epoxy composite tubes under quasi-static axial loading. App. Compos. Mater. **25**, 1401 (2018)

51. M.J. Ghoushji, R. Alebrahim, R. Zulkifli, A.B. Sulong, S. Abdullah, C.H. Azhari, Iranian Poly. J. **27**, 563 (2018)

52. M. Alkateb, S.M. Sapuan, Z. Leman, M. Jawaid, M.R. Ishak, Fib. Poly. **18**, 1187 (2017)

53. M.N. Roslan, M.Y. Yahya, Z. Ahmad, A.H. Abdul Rashid, W.X. Wang, Energy absorption capacity of basalt sandwich composite cylinder subjected to axial compression loadings. Mater. Sci. Forum **917**, 7 (2018)

54. S.A. Oshkovr, S.T. Taher, A.A. Oshkour, A.K. Ariffin, C.H. Azhari, Compos. Struct. **95**, 411 (2013)